10220 *Biochemistry* **2009,** *48,* 10220–10234
DOI: 10.1021/bi901096j

BIOCHEMISTRY
including biophysical chemistry & molecular biology
Article

Kinetics and Thermodynamics of Flip-Flop in Binary Phospholipid Membranes Measured by Sum-Frequency Vibrational Spectroscopy[†]

Timothy C. Anglin and John C. Conboy*

Department of Chemistry, University of Utah, 315 South 1400 East, Salt Lake City, Utah 84112

Received June 29, 2009; Revised Manuscript Received September 9, 2009

ABSTRACT: In order to better characterize the dependence of lipid flip-flop rate and thermodynamics on the nature of the lipid headgroup, we have studied the kinetics of flip-flop for single-lipid and mixed-lipid bilayers consisting of 1,2-distearoyl-*sn*-glycero-3-phosphocholine (DSPC) and 1,2-distearoyl-*sn*-glycero-3-phosphoethanolamine (DSPE) as a function of both pressure and temperature. The kinetics of flipping were studied by sum-frequency vibrational spectroscopy (SFVS), which does not require exogenous chemical labeling of the lipid species of interest. Additionally, SFVS may be employed to track only a single species (DSPE or DSPC) within a binary mixture by selective deuteration of the matrix lipid to make it spectroscopically inactive. Using this approach, we have found the flip-flop of pure DSPE to be slower than the flip-flop of pure DSPC by nearly 2 orders of magnitude. The thermodynamics of the pure systems were analyzed in order to better understand the physical factors underlying their transmembrane dynamics. Headgroup hydrophobicity and associated solvent effects, as well as lipid packing constraints, appear to play a key role in determining the rate of flip-flop for these two species. For mixtures of DSPE + DSPC, both components exhibited similar rates of flip-flop at a given mole fraction of DSPE. The kinetics and thermodynamics of flip-flop in the mixtures did not vary uniformly with changing composition but were well correlated to changes in the molecular packing as a function of DSPE content in the bilayer.

Cellular membranes of eukaryotic cells are comprised of a wide array of phospholipid species. In eukaryotic membranes, phospholipids containing phosphocholine (PC)[1] headgroups are the most common, followed by phosphoethanolamine (PE) (*1*−*4*). Sphingomyelin (SM), phosphatidylserines (PS), and in some membranes phosphatidylinositol (PI) are present at lower concentrations (*1*−*4*). Among the primary headgroups mentioned above, there is also a great deal of diversity with regard to alkyl chain length and degree of saturation (*2*, *5*). Each of these chemically distinct lipids is believed to contribute a different thermodynamic property to the membrane, allowing the cell to tailor membrane physical properties such as fluidity and permeability based on lipid composition and membrane structure (*6*−*9*). However, characterizing the influence of the chemical properties of each of these lipid types on membrane dynamics is a daunting task. Although the phase behavior and lateral diffusion of different membrane lipids are reasonably well understood, characterization of the transmembrane diffusion (flip-flop) of lipids has proven to be especially challenging.

Lipid flip-flop is an essential process in biological membranes. Lipids arriving at the plasma membrane from their site of synthesis must distribute themselves, via flip-flop, across the inner and outer leaflets in order to maintain mass balance across the membrane and accommodate uniform growth of the cell (*10*, *11*). Cellular regulation of flip-flop is also essential to the maintenance of plasma membrane asymmetry, and loss of asymmetry via flip-flop can lead to apoptosis (*4*, *12*−*16*). Unfortunately, the spontaneous rate of flip-flop for native lipid species is not well characterized. Much of the effort to date has focused on elucidating ATP-dependent, protein-driven mechanisms for flip-flop (*17*, *18*), for which there is much conflicting evidence (*11*, *17*, *19*−*21*). While there has been limited progress toward this goal (*19*), it is increasingly clear that enzymatic mechanisms alone cannot account for all flip-flop activity observed in the cell or for the disparity in flip-flop rates observed in different membrane types (*10*, *11*, *20*, *22*). This has led to renewed interest in the spontaneous flip-flop of lipids in biological membranes. It is this spontaneous flipping behavior that we wish to better understand.

Since the first systematic studies of phospholipid flip-flop were undertaken, a wide variety of techniques have been employed to describe the rate of phospholipid flipping, including ESR (*23*−*26*), NMR (*27*), fluorescence (*28*−*35*), small angle neutron scattering (SANS) (*36*), and sum-frequency vibrational spectroscopy (SFVS) (*37*−*40*). Aside from SANS and SFVS, these methods rely on lipid−probe molecules. Such techniques are at a distinct disadvantage, as it is difficult to relate the

[†]Funding provided by NSF Grant 0515940. Any opinions, findings, and conclusions or recommendations expressed in this material are those of the authors and do not necessarily reflect the views of the National Science Foundation.

*Corresponding author. E-mail: conboy@chem.utah.edu. Phone: (801) 585-7957. Fax: (801) 587-9919.

[1]Abbreviations: DSPC, 1,2-distearoyl-*sn*-glycero-3-phosphocholine; DSPE, 1,2-distearoyl-*sn*-glycero-3-phosphoethanolamine; PC, phosphocholine; PE, phosphoethanolamine; SM, sphingomyelin; PS, phosphatidylserine; PI, phosphatidylinositol; ATP, adenosine triphosphate; ESR, electron spin resonance; NMR, nuclear magnetic resonance; SANS, small angle neutron scattering; SFVS, sum-frequency vibrational spectroscopy; PSLB, planar-supported lipid bilayer; T_m, gel to liquid-crystalline phase transition temperature; DSPE-d_{70}, 1,2-distearoyl-D70-*sn*-glycero-3-phosphoethanolamine; LB, Langmuir−Blodgett; LS, Langmuir−Schaeffer; DSPC-d_{70}, 1,2-distearoyl-D70-*sn*-glycero-3-phosphocholine; NBD, (7-nitrobenzo-2-oxa-1,3-diazol-4-yl)aminohexanoate; C_6-NBD-PE, 1-palmitoyl-2-(NBD)hexanoyl-PE; POPC, 1-palmitoyl-2-oleoyl-*sn*-glycero-3-phosphocholine; C_6-NBD-PC, 1-palmitoyl-2-(NBD)-hexanoyl-PC.

 Published on Web 09/11/2009 © 2009 American Chemical Society

behavior of the probe to the native lipid species due to discrepancies in size, charge, polarity, or solubility. Recently, the disparity between the rate of flip-flop for a saturated phosphocholine lipid (1,2-dipalmitoyl-*sn*-glycero-3-phosphocholine) and a spin-labeled analogue was described (*40*). The difference in rates was substantial and exemplifies the pitfalls of using modified probes to measure flip-flop, as they do not always represent the behavior of their unmodified analogue. Nakano et al. have described a method for measuring flip-flop of isotopically substituted phospholipids using SANS (*36*). While the use of isotopically labeled lipids avoids many of the issues of chemical labeling that are found in fluorescent and spin-labeled techniques (*41*), the dependence of their method on vesicle solutions still requires simultaneous measurement of transmembrane and intermembrane lipid transfer and remains an indirect measurement of lipid flip-flop. We have recently demonstrated the utility of SFVS as a method for directly tracking phospholipid flip-flop in planar-supported lipid bilayers (PSLBs) which avoids many of the complications discussed above (*39*, *40*).

SFVS has proven advantageous for its ability to measure flip-flop kinetics without the use of probe molecules. Our laboratory has previously characterized the kinetics and thermodynamics of flip-flop for PC lipids in the gel phase, as a function of chain length, lateral pressure, and temperature (*37*, *40*). The influence of small peptides and cholesterol on the dynamics of PC bilayers has also been investigated, and the body of work performed by this method is steadily growing (*38*, *42*). However, the majority of systems in which lipid flip-flop has been measured by SFVS were comprised of a single class of phospholipid species, namely, saturated phosphatidylcholines. In order to better understand the process of spontaneous flip-flop in cellular membranes, it is necessary to expand the previous work to more relevant and complex membrane compositions. Our initial steps in this direction included a systematic study of the dependence of flip-flop rate on the chain length for a series of homologous saturated PC species (*40*).

In this study, we have investigated the influence of headgroup chemical identity on lipid flip-flop dynamics for both single component bilayers and binary phospholipid mixtures. 1,2-Distearoyl-*sn*-glycero-3-phosphoethanolamine (DSPE) and 1,2-distearoyl-*sn*-glycero-3-phosphocholine (DSPC) were chosen as model lipids for this study. Phosphocholine- and phosphoethanolamine-derived phospholipids are typically the most prevalent phospholipid types encountered in biological membranes. DSPC was selected as a model phosphocholine-type lipid because an abundance of kinetic and thermodynamic data for this lipid species has already been collected (*1*, *4*, *40*). DSPE is an attractive complement to DSPC as the two are structurally homologous with respect to their alkyl chains and vary only in the presence (DSPC) or absence (DSPE) of methyl substituents on the terminal amine of the headgroup. Although methylation of the terminal amine of the lipid headgroup is a minor variation on lipid structure, it is an important chemical modification which alters the size, hydrogen bonding, and polarity of the molecule. Specifically, DSPE is capable of acting as both a hydrogen bond donor via the headgroup amine and a hydrogen bond acceptor via the phosphate group. DSPC, however, has only the phosphate group as a hydrogen bond acceptor and is not capable of acting as a hydrogen bond donor (*6*). The capacity for efficient hydrogen bonding in DSPE has important structural consequences for bilayers composed of that species. Relative to DSPC, DSPE has a more tightly packed structure and a higher gel to liquid-crystalline phase transition temperature (T_m), due to the smaller headgroup size and greater number of attractive interactions that result from hydrogen bonding between adjacent lipid molecules (*43*). In what follows, we present the kinetics and thermodynamics of flip-flop for DSPE phospholipid bilayers as well as the dynamics for each component in mixed bilayers of DSPE and DSPC. In addition to characterizing the role of the lipid headgroup in determining the kinetic and thermodynamic behavior of simple lipid membranes and lipid mixtures, this work will demonstrate the utility of SFVS for interference-free measurement of the dynamics of individual lipid components within a mixed bilayer system without requiring exogenous chemical modification of the lipid.

SFVS Spectroscopy of PSLBs. The underlying theory of SFVS and the specifics of its application to the measurement of membrane structure and dynamics have been detailed in several earlier publications (*40*, *44*), and only the salient aspects of the method will be reviewed here. SFVS is performed by temporally and spatially overlapping a fixed visible and a tunable IR laser source at the bilayer interface where they interact with the sample and produce coherent radiation at the sum of the input frequencies:

$$\omega_3 = \omega_1 + \omega_2 \tag{1}$$

The intensity at ω_3 is proportional to the square of the second-order susceptibility (χ^2) of the molecules at the interface:

$$I_{SFVS} \propto |\chi^2|^2 \tag{2}$$

which has both resonant and nonresonant ($\chi_{NR}{}^2$) contributions, expressed as

$$\chi^2 = \sum_\nu \frac{N\langle A_i M_{jk}\rangle}{\omega_\nu - \omega_{IR} - i\Gamma_\nu} + \chi_{NR}{}^2 \tag{3}$$

The resonant contribution depends on the number of molecules at the interface (N), the IR (A_i) and Raman (M_{jk}) transition probabilities, and the line width (Γ_ν) of the vibrational transitions at frequencies (ω_ν) as a function of the input IR radiation (ω_{IR}). An important aspect of the SFVS process is the dependence of the intensity upon the relative orientation of the dipoles; mathematically, this is expressed by the *bra* ($\langle$) and *ket* ($\rangle$) notation used in eq 3, indicating the ensemble orientational average of the IR and Raman transition dipole moments. The transition dipole moments of oppositely oriented molecules will be out of phase with one another. Due to the coherent nature of the SFVS process, these out of phase elements will destructively interfere and no signal will be observed.

This symmetry constraint allows one to study phospholipid dynamics in PSLBs using SFVS. PSLBs are inherently symmetric structures, with well-oriented phospholipid molecules lying along both the positive and negative axes of the surface normal (*44*). Considering the symmetry constraints discussed above, this should, and does, lead to effective cancellation of the SFVS signal when both leaflets of the bilayer are composed of the same lipid (*44*). However, preparation of a bilayer which is asymmetric with respect to the vibrational transitions of the component species in each leaflet removes the cancellation between the two leaflets and gives rise to considerable SFVS signal. This is best accomplished by preparing a bilayer with an unmodified (native) phospholipid in one leaflet and using a perdeuterated analogue of the same species in the opposite leaflet of the bilayer. These two phospholipids will be chemically identical, yet the vibrational

transitions for the deuterated and protiated lipids will lie at different frequencies, creating the asymmetry necessary to generate a SFVS signal. This principle is illustrated in Figure 1, which shows the SFVS spectrum for an asymmetric bilayer consisting of DSPE in the proximal leaflet and 1,2-distearoyl-D70-*sn*-glycero-3-phosphoethanolamine (DSPE-d_{70}) in the distal leaflet (green), as well as a symmetric bilayer consisting of an equimolar mixture of DSPE and DSPE-d_{70} in each leaflet (pink). The resonances due to DSPE are clearly seen in the spectrum of the asymmetric bilayer, while the symmetric bilayer has very little signal due to cancellation of the dipoles in the opposing leaflets (Figure 1, inset). If an asymmetric bilayer is allowed to undergo flip-flop, the composition of the bilayer will become increasingly symmetric due to the movement of lipids between the leaflets. By tracking the changes in the SFVS signal over time at a fixed infrared frequency, it is possible to directly monitor these changes in the bilayer symmetry in real time, thereby providing a means to measure the rate of phospholipid flip-flop.

Kinetics of Lipid Flip-Flop Measured by SFVS. The terminal methyl symmetric stretching vibration (CH_3 ν_s) at 2875 cm^{-1} from the phospholipid alkyl chains is an excellent indicator of bilayer symmetry as the dipole moment of this vibration lies primarily along the bilayer normal (*44*) and is the most dominant feature in the SFVS spectrum. The component of the second-order susceptibility tensor specific for the CH_3 ν_s of the lipids in the bilayer may be expressed as

$$\chi^2 = \frac{N_{\text{distal}}}{\varepsilon_0}\langle\beta^{CH_3\nu_s}\rangle - \frac{N_{\text{proximal}}}{\varepsilon_0}\langle\beta^{CH_3\nu_s}\rangle \quad (4)$$

where N_{distal} and N_{proximal} represent the fraction of protiated lipids in the distal and proximal leaflet, respectively, $\beta^{CH_3\nu_s}$ is the hyperpolarizability for the CH_3 ν_s vibration, and ε_0 is the vacuum permittivity. Equation 4 shows the dependence of the nonlinear susceptibility on the distribution of lipids in the two leaflets of the bilayer, where the negative sign describes the destructive interference that occurs as a consequence of the opposing orientation for lipids in opposing leaflets. By substitution of eq 4 into eq 2, it is possible to describe the dependence of the SFVS signal upon the fraction of protiated lipids in each leaflet according to

$$I_{CH_3}(t) \propto (N_{\text{distal}} - N_{\text{proximal}})^2 \quad (5)$$

From eq 5 it is possible to derive an integrated rate expression relating the decay in SFVS intensity to the rate of lipid flipping (derived elsewhere) (*40*). Assuming a unimolecular mechanism, the rate expression for flip-flop is given as (*40*)

$$I_{CH_3}(t) = I_{\max}e^{-4kt} + I_0 \quad (6)$$

where k is the rate constant for flip-flop, $I_{CH_3}(t)$ is the time-dependent SFVS intensity, $I_{\max}$ is the maximum resonant SFVS signal, and I_0 represents the baseline offset due to nonresonant signal and instrument offset. By measuring the change in SFVS signal intensity as flip-flop occurs, it is possible to determine the rate constant (k) for phospholipid flip-flop in PSLBs. Examination of the dependence of k on the lateral pressure and temperature of the lipid bilayer may also be used to characterize the thermodynamic barrier to flip-flop (*45*).

Thermodynamics of Flip-Flop in PSLBs. Using transition state theory, the free energy of activation for lipid flip-flop in PSLBs is determined by measuring the rate of flip-flop over a range of temperatures and fitting the observed rate constants (k) according to

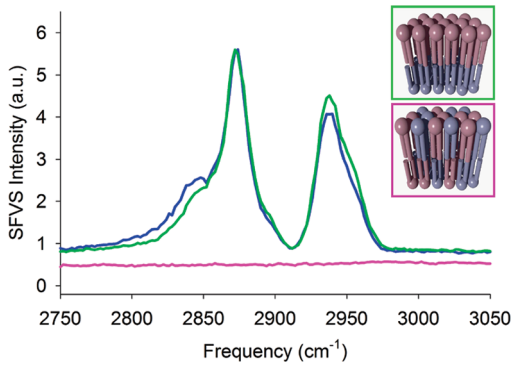

FIGURE 1: SFVS spectra for an asymmetric DSPE:DSPE-d_{70} bilayer (green). The peaks are assigned as the CH_2 symmetric stretch (ν_s) at 2848 cm^{-1}, the CH_3 ν_s at 2875 cm^{-1}, the CH_2 Fermi resonance (FR) at 2905 cm^{-1}, the CH_3 FR at 2938 cm^{-1} and the CH_3 antisymmetric stretch (ν_{as}) at 2967 cm^{-1} (*40*). After complete flip-flop of the bilayer at elevated temperature and subsequent cooling, the SFVS spectrum shows no features due to the destructive interference from protiated lipids in both leaflets (pink). The spectrum of an asymmetric DSPE:DSPE-d_{70} bilayer (green) is nearly identical to that for a DSPC:DSPC-d_{70} bilayer (blue), as both bilayers have the same alkyl chain structure. The spectra and spectral fits are offset for clarity. Inset: Illustrations of asymmetric (green) and symmetric bilayers (pink).

$$k = \frac{k_B T}{h}e^{-\Delta G^{\ddagger}/RT} \quad (7)$$

where k_B is Boltzman's constant, T is the temperature in kelvin, R is the gas constant, h is Planck's constant, and $\Delta G^{\ddagger}$ is the free energy barrier to phospholipid flip-flop (*46*, *47*). Equation 7 can be expressed in terms of the Arrhenius activation energy E_a, the reversible work required to reach the transition state ($\Pi\Delta a^{\ddagger}$), and the entropy of activation ($\Delta S^{\ddagger}$):

$$k = \frac{k_B T}{h}e^{(-E_a/RT)-(\Pi\Delta a^{\ddagger}/RT)+(T\Delta S^{\ddagger}/RT)+1} \quad (8)$$

The Arrhenius activation energy (E_a) and preexponential factor (A) are determined from the temperature dependence of the rate of flipping according to the Arrhenius equation, given as

$$\ln k = \ln A - \frac{E_a}{RT} \quad (9)$$

Plotting ln k for a given lipid as a function of $1/T$ provides E_a from the slope and A from the intercept of the data.

In order to determine $\Pi\Delta a^{\ddagger}$ and $\Delta S^{\ddagger}$, one must also determine the lateral pressure dependence of the rate of flip-flop. These pressure-dependent kinetic measurements are not readily achieved with vesicle-based systems, as very large external pressures (~2 kbar) are required to alter the lateral pressure within vesicles in solution (*48*). However, the lateral pressure in PSLBs may be easily accomplished using LB/LS deposition techniques. Demonstration of the pressure control afforded by this technique may be found in previous publications (*37*, *45*). The activation area ($\Delta a^{\ddagger}$) is calculated from the dependence of ln k on the lateral pressure of the film (Π) at a given temperature according to

$$-RT\left(\frac{\partial \ln k}{\partial \Pi}\right)_T = \Delta a^{\ddagger} \quad (10)$$

The area of activation, $\Delta a^{\ddagger}$, represents the area per molecule expansion required for a phospholipid to reach the transition state (*37*). The work required to reach the transition state is given by the product of the activation area and lateral surface pressure ($\Pi\Delta a^{\ddagger}$). It should be noted that two-dimensional pressure, activation area, and work terms are used here in place of their three-dimensional analogues. The treatment of bilayers as two-dimensional thermodynamic systems is well established and reflects the two-dimensional nature of the intermolecular interactions for the species comprising the film (*49*−*52*).

Finally, the entropy of activation may be calculated from the Arrhenius preexponential factor and the work term by

$$\Delta S^{\ddagger} = R\left(\ln\left(\frac{Ah}{k_B T}\right) + \left(\frac{\Pi\Delta a^{\ddagger}}{RT}\right) - 1\right) \quad (11)$$

Accurate calculation of $\Delta S^{\ddagger}$ therefore requires knowledge of both the pressure and temperature dependence of the rate of flip-flop for a given lipid species or mixture.

Given adequate knowledge of the kinetics of flipping, a straightforward determination of the net free energy barrier ($\Delta G^{\ddagger}$) and the contributions to the energy barrier due to E_a, $\Pi\Delta a^{\ddagger}$, and $\Delta S^{\ddagger}$ is thus possible, where the complete free energy barrier to flip-flop is given as

$$\Delta G^{\ddagger} = E_a - RT + \Pi\Delta a^{\ddagger} - T\Delta S^{\ddagger} \quad (12)$$

Detailed derivation of each of the thermodynamic expressions used above is presented in greater detail elsewhere (*45*).

In the work presented here, we describe the preparation and study of DSPE bilayers and of mixed DSPE−DSPC bilayers. Careful comparison of the activation thermodynamics for DSPE and DSPC in these bilayers provides an avenue to relate the chemical properties of the lipid headgroup to specific energetic aspects of the flip-flop transition state (entropy, work, or enthalpy, for instance).

MATERIALS AND METHODS

DSPC, DSPE, 1,2-distearoyl-D70-*sn*-glycero-3-phosphocholine (DSPC-d_{70}), and DSPE-d_{70} were purchased from Avanti Polar Lipids (Alabaster, AL) and used without further purification. Spectral grade chloroform and methanol were obtained from Mallinckrodt (Phillipsburg, NJ) and Sigma-Aldrich (St. Louis, MO), respectively, and were used as received. Nanopure water (Barnstead Thermolyne, Dubuque, IA) with a minimum resistivity of 18.2 MΩ·cm was used for all sample preparation. D_2O was purchased from Cambridge Isotope Laboratories (Andover, MA) and passed through a 0.20 μm syringe filter prior to use.

Bilayer Preparation. Phospholipid samples were prepared by dissolving the appropriate lipid in a 65:35:1 ratio mixture of chloroform:methanol:water to a concentration of 1 mg/mL. Mixtures of phospholipids were prepared by mixing these solutions at the appropriate ratios.

The PSLB substrates for use in this study were hemicylindrically fused silica prisms (Almatz Optics, Marlton, NJ). Prior to bilayer formation, the prisms were cleaned using 70% H_2SO_4−30% H_2O_2. (Note: This solution is a strong oxidizer and reacts violently with organic materials. Appropriate safety precautions such as acid-resistant gloves and proper shielding should be used during handling.) The substrate prism was then rinsed with copious amounts of nanopure water. Final cleaning of the fused silica prism was accomplished by plasma cleaning in an argon plasma for 2−5 min.

PSLBs were prepared by the Langmuir−Blodgett (LB)/Langmuir−Schaeffer (LS) deposition method using a KSV Instruments minitrough (Helsinki, Finland). The LB trough was filled with a subphase of nanopure water before submerging the prism. In some instances, the pH of the subphase required adjustment to pH = 7.0 ± 0.3 using dilute NaOH (Mallinckrodt, Phillipsburg, NJ). No significant experimental differences were noted between samples prepared from the two subphase compositions. After allowing for stabilization of the Wilhelmy plate balance, the phospholipid solutions in chloroform were carefully spread at the air−water interface of the trough, and the solvent was allowed to evaporate for a minimum of 15 min. The phospholipid monolayer was then compressed to the desired pressure by Teflon barriers and allowed to equilibrate for a minimum of 15 min, after which the substrate was slowly withdrawn while pressure was maintained via feedback from the Wilhelmy plate balance to the barrier motors. Following deposition of the first layer (LB deposition), the trough was cleaned, and a new phospholipid solution was spread at the air−water interface of the trough. Following equilibration and compression of the monolayer as described previously, the prism with a lipid monolayer deposited on the surface was transferred through the interface into the subphase in a horizontal orientation (LS layer deposition). After the bilayer was deposited onto the substrate, the sample was transferred to a custom Teflon sample cell while maintaining the bilayer in an aqueous environment.

DSPE bilayers (DSPE or DSPE-d_{70}) were prepared at pressures of 15, 30, and 40 mN/m in order to determine the pressure dependence of DSPE flip-flop. For all mixed DSPE and DSPC bilayers, the sample deposition pressure was 30 mN/m. The choice of pressure in the mixed bilayers is motivated by the fact that 30 mN/m is thought to be the lateral pressure which best represents biological membrane systems (*51*).

Measurement of Lipid Flip-Flop Rates. After assembly of the prism and bilayer sample into the flow cell, D_2O was flushed through the cell in order to eliminate any spectral interference between H_2O and the phospholipid molecules. The sample cell was placed into the instrumental setup and aligned for maximum SFVS signal. The SFVS instrumentation consisted of a custom-built LaserVision OPO/OPA (Laservision, Bellvue, WA) pumped by a 10 Hz, nanosecond-pulsed Nd:YAG laser (Continuum, Santa Clara, CA) with a pulse duration of ∼5−7 ns. The laser sources were directed to the silica−water interface in a total internal reflection geometry, which leads to signal enhancement at the interface where the bilayer sample is located (*53*−*55*). The SFVS output was spatially separated from the input beams, and stray laser light was rejected by interference and bandpass filters prior to detection of the output with a photomultiplier tube. Data were recorded with Labview software (National Instruments, Austin, TX) using a gated integrator and boxcar averager for signal processing and collection.

An initial spectrum was obtained prior to measuring the kinetics of flip-flop in order to verify bilayer formation. The spectrum was collected by scanning the IR frequency from 2750 to 3100 cm^{-1} in 2 cm^{-1} steps and averaging 30 pulses per step. After obtaining a spectrum, the spectrometer was tuned to 2875 cm^{-1} for the measurement of flip-flop kinetics. The rate constant (k) for flip-flop was determined by elevating the temperature of the cell and monitoring the change in SFVS signal at 2875 cm^{-1} over time and then fitting the observed signal decay using eq 6.

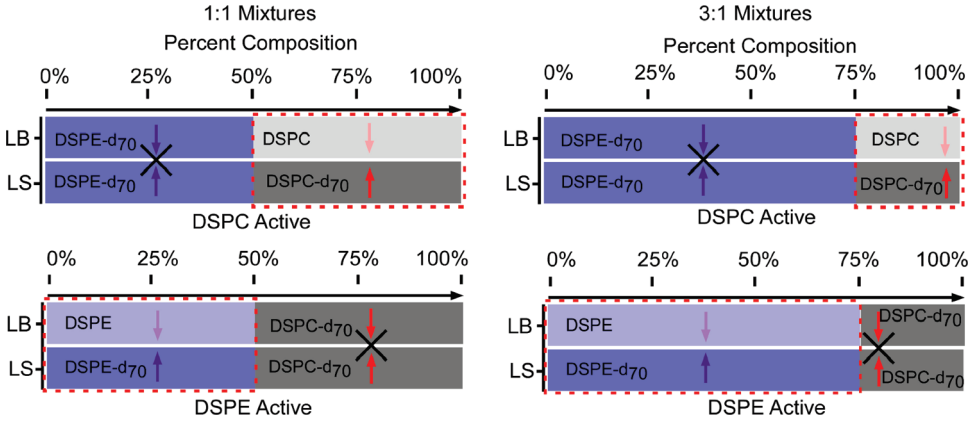

FIGURE 2: An illustration of the isolation of the SFVS signal from a single component of a binary lipid mixture. Blue boxes represent DSPE lipid species, while gray boxes represent DSPC lipids. Shading of the boxes corresponds to the deuterated or protiated analogue of each lipid type. For each nominal concentration (50% DSPE or 75% DSPE, in this case), a particular combination of deuterated and protiated lipids may be chosen such that the DSPE or DSPC component is responsible for the SFVS signal.

Temperature control for the sample cell was managed using a thermoelectric Peltier element incorporated into the rear of the sample cell and separated from the sample volume by a thin Teflon divider. The temperature was monitored by means of a thermistor located in the sample solution volume immediately adjacent to the sample surface. The thermistor also provided temperature feedback for control of the thermoelectric heating unit in order to ensure stable and accurate temperature control.

Flip-Flop Kinetics in Binary Lipid Mixtures. Mixed bilayers of DSPE and DSPC were also prepared using the LB/LS method as described above. In order to independently characterize the behavior of each species in the complex mixture, it is necessary to prepare bilayers which contain the appropriate combination of deuterated or protiated phospholipids. This ensures that the SFVS signal arises from only one component of the bilayer mixture. As an example, a bilayer consisting of 25% DSPE:75% DSPC-d_{70} in the proximal leaflet and 25% DSPE-d_{70}:75% DSPC-d_{70} in the distal leaflet will result in SFVS signal from only the protiated 25% DSPE component. This allows for interference-free tracking of the SFVS signal for the DSPE component in a mixture of DSPE and DSPC. In order to determine the behavior of the DSPC component of the same mixture, the proximal leaflet may instead be prepared with 25% DSPE-d_{70} and 75% DSPC with the same distal leaflet composition as before. In this way, the behavior of each component of the mixture may be individually determined without interference from the other species. A graphic illustrating this approach appears in Figure 2. In this figure, the lipid type (PE or PC) is designated by color (blue or gray respectively), while the isotopic composition is indicated by shading. The cancellation of signal occurs when the isotopic composition for a given lipid type is the same in each leaflet, while the lipid type is "spectroscopically active" if the isotopic composition varies between the two leaflets. In the examples provided, bilayers consisting of 3:1 and 1:1 DSPE:DSPC ratios are shown with the isotopic composition varied such that either the DSPE or DSPC component may be observed. A similar approach is utilized for other DSPE:DSPC ratios.

Pressure−Area Isotherms. Pressure−area isotherms were collected for DSPC, DSPE, and each DSPC + DSPE mixture in order to determine the packing behavior in these bilayers. Phospholipid solutions containing DSPE, DSPC, or the DSPE + DSPC mixtures were carefully spread at the air−water interface of the LB trough, and the solvent was allowed to evaporate. Following an appropriate equilibration period, the sample was compressed by Teflon barriers while a Wilhemy plate balance was used to measure the pressure, which was recorded by the control software. A minimum of three isotherms were collected for each sample. The area per molecule for each sample was determined by averaging the recorded area per molecule at 30 mN/m from all measured isotherms.

RESULTS

SFVS Spectra of DSPE and DSPE + DSPC Bilayers. Figure 1 shows the SFVS spectrum for a DSPE−DSPE-d_{70} bilayer in D_2O. The SFVS spectrum for a DSPE−DSPE-d_{70} bilayer is essentially identical to that found for DSPC−DSPC-d_{70} bilayers (Figure 1). The resonances observed in the spectra presented in Figure 1 correspond to the CH_2 symmetric stretch (ν_s) (2848 cm^{-1}), the terminal methyl CH_3 ν_s (2875 cm^{-1}), the CH_2 Fermi resonance (FR) (2905 cm^{-1}), the CH_3 FR (2938 cm^{-1}), and the CH_2 antisymmetric stretch (ν_{as}) (2960 cm^{-1}) (*44*). The last two of these resonances appear as a combination band centered near 2950 cm^{-1}. The SFVS spectra of DSPC and DSPE are dominated by features arising from the alkyl chains rather than the headgroup (*44*). Thus similar spectral results are expected for DSPE and DSPC due to the identical structure of the fatty acid chains for each lipid. N−H stretching modes are not observed in the SFVS spectrum of DSPE due to the rapid deuterium exchange between the lipid and solvent (*56*). For DSPE + DSPC mixtures, the spectra were similar to those for the pure bilayers, differing only in total intensity according to the varying number of spectroscopically active species in each mixed bilayer.

DSPE and DSPE + DSPC Flip-Flop Kinetics. For pure DSPE bilayers, the kinetics of flip-flop were measured as a function of both pressure and temperature to determine the contributions to the flip-flop free energy barrier due to pressure work, enthalpy, and entropy. Decays were collected for DSPE−DSPE-d_{70} at pressures from 15 to 40 mN/m and temperatures ranging from 51.0 to 70.0 °C. Representative decays illustrating the pressure dependence of the decay rate at 61 °C are shown in Figure 3. For each temperature and pressure combination examined, the rate constant for flip-flop was determined by fitting the decays using eq 6. A summary of the rate constants for DSPE flip-flop as a function of pressure and temperature is

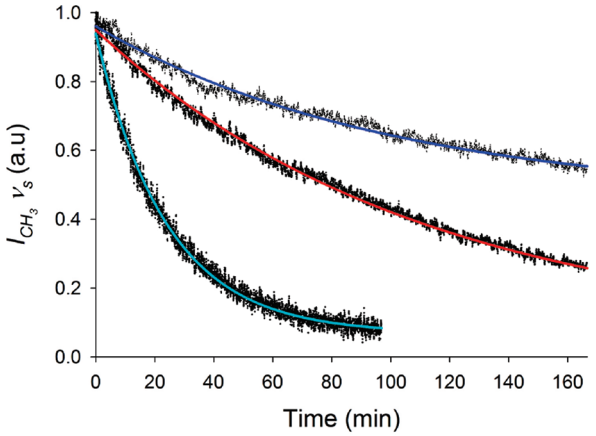

FIGURE 3: SFVS decays for DSPE−DSPE-d_{70} bilayers at ~61 °C and 40 mN/m (blue), 30 mN/m (red), and 15 mN/m (cyan). The raw data are shown in black, and the fit to the data, using eq 6, is shown in the solid lines. The x-axis is truncated in order to better illustrate the difference in decay rates, yet all decays were monitored over a sufficient time period to ensure decay of the SFVS signal to baseline.

presented in Table 1. Table 1 also lists the half-life for decay, given as

$$t_{1/2} = \frac{\ln 2}{2k} \tag{13}$$

The variation in DSPE flip-flop rate as a function of both temperature and pressure is illustrated in Figure 4, which shows the Arrhenius plots for DSPE−DSPE-d_{70} bilayers at 15, 30, and 40 mN/m. The large error bars represent variations in pooled data from replicate measurements whereas single measurements have an error determined from the kinetic fitting. All errors are reported to a single standard deviation.

The rate of lipid flip-flop was also measured in mixed DSPE + DSPC bilayers prepared with DSPE mole fractions (x_{DSPE}) of 0.10, 0.25, 0.50, and 0.75. For all mixtures, except x_{DSPE} = 0.10, the kinetics for both DSPE and DSPC were measured by careful selection of the protiated or deuterated components. Only the behavior of DSPC was monitored in the x_{DSPE} = 0.10 bilayer (90% DSPC:10% DSPE-d_{70}) mixtures, due to the low signal for DSPE in 10% DSPE:90% DSPC-d_{70} bilayers. The kinetics of lipid flip-flop for DSPC and DSPE in the mixed bilayers followed a single exponential decay in all cases and were well fit by eq 6. Representative SFVS decays are shown in Figure 5 for lipid mixtures at 47.0 °C as a function of DSPE concentration. The rate constants and half-life of decay for each component of the mixed bilayers at the various compositions examined are summarized in Table 2. Unlike the pure DSPE bilayers presented above, the mixed bilayers were examined only at lateral pressures of 30 mN/m. Due to the large number of samples to be studied, it was not practical to examine the temperature dependence of each mixture at numerous pressures. As noted above, 30 mN/m was chosen for these mixtures, as this is thought to be the lateral pressure which best represents biological membrane systems (*51*). The range of temperatures over which the decays were collected varied for each sample set and was determined by the rates which could be reasonably measured using our SFVS method. The upper rate limit is determined by the need to reach a stable temperature prior to complete decay of the signal, while the lower limit is determined by the requirement for sufficient sample throughput.

The kinetics of flip-flop in the mixed DSPC + DSPE bilayers did not vary in a systematic fashion as a function of membrane composition. The rate of DSPC flip-flop in the mixed bilayers undergoes an initial increase at low mole fractions of DSPE. The half-life of DSPC flip-flop for bilayers consisting of x_{DSPE} = 0.10 is 11.0 ± 0.1 min at 47.0 °C, while $t_{1/2}$ = 52 ± 6 min for pure DSPC at the same temperature (*45*). This initial increase in flip-flop rate occurs despite the observation that pure DSPE exhibits a slower rate of flipping than pure DSPC at the same temperature and pressure. For x_{DSPE} = 0.25 at 47.0 °C, the flip-flop kinetics of both the DSPE and DSPC species are slightly slower ($t_{1/2}$ ~99 min) than the rates found for the pure DSPC system, reflecting a decrease in the flip-flop rate relative to x_{DSPE} = 0.10. The rates of flip-flop continue to slow as the DSPE concentration

Table 1: Kinetics of DSPE Flip-Flop as a Function of Surface Pressure and Temperature[a]

Π (mN/m)	temp (°C)	k (s^{-1}) × 10^5	$t_{1/2}$ (min)
40	61.0	1.27	454
	63.0	2.07	280
	65.0	4.03	143
	67.0	5.86	98
30	58.0	1.78	325
	60.0	2.99	193
	61.1	6.12	94
	65.0	13.4	43
	68.0	22.0	26
	70.0	34.0	17
15	51.0	1.40	412
	53.0	2.35	246
	55.0	7 ± 4	90 ± 50
	56.0	6.64	87
	58.0	8 ± 3	70 ± 30
	60.0	16.61	35

[a]The error in temperature for each experiment is ±0.1−0.2 °C and that for the surface pressure is ±0.2 mN/m. The error in the determined rate constant is typically ~1% for a given determination. Where reported, larger errors represent the error in pooled data for several decays measured at a common temperature.

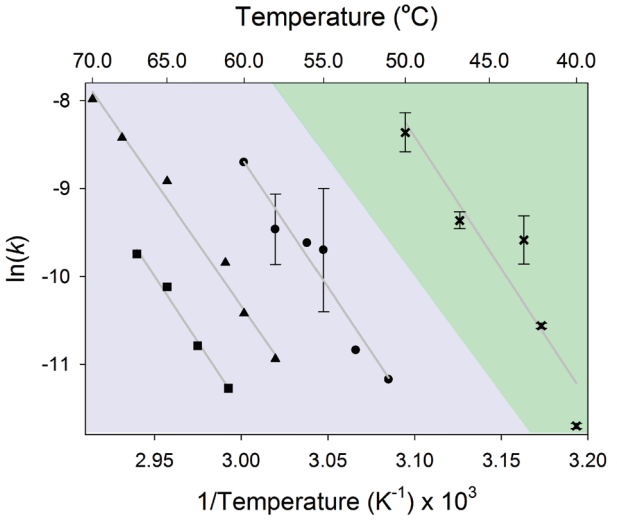

FIGURE 4: Arrhenius plots for DSPE flip-flop at 15 mN/m (●), 30 mN/m (▲), and 40 mN/m (■) prepared from the data listed in Table 1. The error bars represent the error in pooled data for a given temperature. For comparison, the Arrhenius behavior for DSPC flip-flop at 30 mN/m, as determined in a previous study, is also shown (×) (*40*).

increases. Mixed bilayers with high mole fractions of DSPE ($x_{DSPE} = 0.75$) exhibit kinetic behavior intermediate to the results obtained for $x_{DSPE} = 0.50$ and $x_{DSPE} = 1$. The DSPE component of the mixtures undergoes flip-flop with a rate similar to that of the DSPC component for $x_{DSPE} = 0.25$, 0.50, and 0.75. Arrhenius plots for each mixture are presented in Figure 6. The overlap in the Arrhenius plots for the DSPC and DSPE components of the mixtures with $x_{DSPE} = 0.25$, 0.50, and 0.75 illustrates the common kinetic behavior for each species within the mixture.

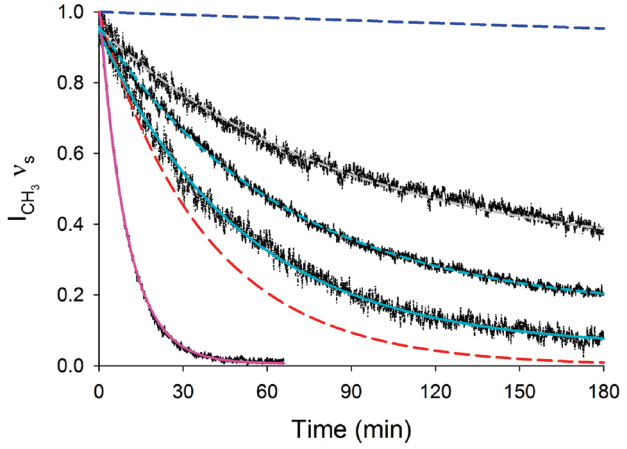

FIGURE 5: Representative DSPC flip-flop decays illustrating the dependence of flip-flop kinetics on DSPE concentration. The decay of the CH_3 ν_s recorded at 47 °C for bilayers prepared at 30 mN/m is shown for bilayers consisting of 10% DSPE-d_{70}:90% DSPC (solid pink), 25% DSPE-d_{70}:75% DSPC (solid cyan), 25% DSPE:75% DSPC-d_{70} (dashed cyan), and 50% DSPE:50% DSPC-d_{70} (gray). (All concentrations refer to LB leaflet composition; see text.) The raw data are presented in black, with colored lines representing the fits to the data according to eq 6. For comparison, the calculated rates of decay for pure DSPC (red dash) and pure DSPE bilayers (blue dash) are also shown.

Pressure−Area Isotherms for DSPE and DSPE + DSPC Bilayers. Pressure−area isotherms for DSPE, DSPC, and mixed DSPE + DSPC LB monolayers were measured in order to determine the dependence of the lipid packing density upon membrane composition, as the lipid packing density is known to affect the flip-flop kinetics and transition state thermodynamics (*37*, *45*, *48*). Representative pressure−area isotherms for these bilayers are presented in Figure 7 as a function of x_{DSPE}. The mean molecular area for each mixture is determined at 30 mN/m from the isotherm data and is shown graphically in Figure 7 (inset). Relative to pure DSPC, the lipid packing in the DSPC + DSPE mixtures undergoes an initial expansion at $x_{DSPE} = 0.10$, increasing from an initial value of 45.9 ± 1.4 Å^2/molecule for pure DSPC at 30 mN/m to a value of 48.8 ± 0.4 Å^2/molecule. The area per lipid then decreased monotonically for $x_{DSPE} = 0.25$, 0.50, 0.75, and 1.0 with measured areas of 45.4 ± 1.7, 44.0 ± 1.0, 42.4 ± 1.8, and 38.4 ± 0.6 Å^2/molecule, respectively. Other researchers have also noted deviations from ideal packing behavior for DSPE−DSPC mixtures, particularly at DSPE mole fractions of $x_{DSPE} = 0.10$ (*43*).

Table 2: Summary of the Temperature-Dependent Flip-Flop Kinetics for Mixed DSPE−DSPC Bilayers at 30 mN/m as a Function of DSPE Concentration[a]

	temp (°C)	k (s^{-1}) × 10^5	$t_{1/2}$ (min)		temp (°C)	k (s^{-1}) × 10^5	$t_{1/2}$ (min)
100% DSPE	58.0	1.78	325	10% DSPE-d_{70}	40.0	2.71	213
	60.0	2.99	193		40.0	5.02	115
	61.1	6.12	94		42.0	6.42	90
	65.0	13.4	43		44.0	21.7	27
	68.0	22.0	26		44.0	12.5	46
	70.0	34.0	17		46.0	39.0	15
					46.0	27.5	21
					47.0	43.9	13
					48.0	52.6	11
25% DSPE	44.0	5.55	104	25% DSPE-d_{70}	44.0	3.57	162
	47.0	8.03	72		47.0	5.83	99
	49.0	16.8	34		49.0	11.1	52
50% DSPE	46.8	1.85	313	50% DSPE-d_{70}	46.8	1.01	570
	47.0	1.83	315		49.0	2.49	232
	48.0	2.12	272		52.5	16.4	35
	50.0	3.50	165		53.0	36.3	16
	53.0	21.0	27		53.0	21.0	28
	54.0	33.5	17				
75% DSPE	51.0	1.85	313	75% DSPE-d_{70}	51.0	1.85	313
	53.0	1.76	329		53.0	2.28	254
	54.5	12.2	47		55.0	8.27	70
	56.0	3.36	172		55.0	13.0	45
	57.5	15.7	37		58.5	12.3	47

[a]For each mixture, the kinetics of both DSPC and DSPE were determined. Where a concentration for DSPE-d_{70} is noted, the reported kinetics reflect flip-flop of the DSPC component. The errors in k are approximately 1%.

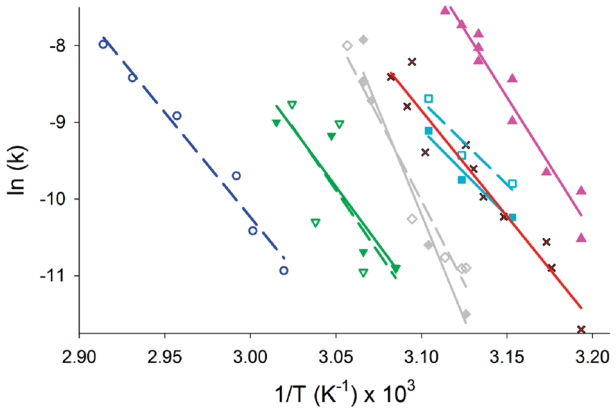

FIGURE 6: Arrhenius plots for mixed DSPE−DSPC bilayers. The nominal concentrations vary by color from 100% DSPC (red) to 10% DSPE (pink), 25% DSPE (cyan), 50% DSPE (gray), 75% DSPE (green), and 100% DSPE (blue). Open symbols refer to the kinetics for the DSPE component of mixed bilayers, while closed symbols refer to the DSPC component of the mixed bilayers. The Arrhenius data for 100% DSPC bilayers were determined in a previous SFVS study (*40*).

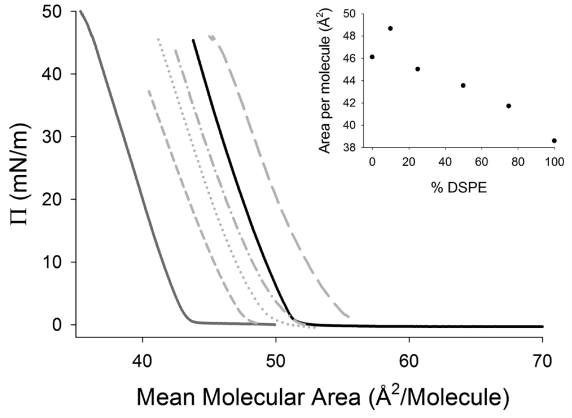

FIGURE 7: Representative pressure area isotherms for mixed DSPE−DSPC bilayers. The concentrations presented above are for 100% DSPC (solid black), 10% DSPE (long gray dash), 25% DSPE (gray dash-dot), 50% DSPE (dotted), 75% DSPE (short gray dash), and 100% DSPE (solid gray). Inset: Variation in mean molecular area as a function of DSPE concentration.

DISCUSSION

DSPE Flip-Flop Kinetics. The rates of DSPE flip-flop presented in the Results section above may be compared to those for pure DSPC in order to describe the influence of the headgroup on the kinetics of lipid exchange. Examination of the rate data for DSPE reveals that the rate of flip-flop is strongly dependent on temperature, as was previously observed for a number of saturated phosphocholines (*40*, *45*). For example, a half-life of 325 min was measured at 58 °C compared to only 17 min at 70.0 °C for a DSPE bilayer prepared at 30 mN/m. However, the rate of flip-flop for DSPE is much slower than the rate previously observed for DSPC flip-flop under similar conditions, and higher temperatures were required to elicit rapid flip-flop. For instance, while the half-life for flip-flop of DSPE at 58.0 °C and 30 mN/m was several hours, the rate of flip-flop for DSPC is too rapid to directly measure under these conditions ($t_{1/2}$(calc) < 100 s) (*40*). The slower rates of flip-flop for DSPE can be attributed to the increased affinity between neighboring DSPE molecules in the bilayer, relative to DSPC. This is due to the smaller headgroup size, which allows closer packing of the lipids and greater van der Waals forces, as well as any hydrogen bonding which may be present between neighboring DSPE molecules or between the surrounding solvent and the lipid headgroup. These attractive interactions are also manifest in other physical properties of the bilayer, such as an elevated gel to liquid-crystalline phase transition temperature for DSPE (T_m = 74.5 °C) relative to DSPC (T_m = 50.5 °C) (*57*).

The pressure dependence of the DSPE flip-flop rate provides insight into the relationship between molecular packing and the propensity for lipid flip-flop. A slower flip-flop rate is expected at higher pressure, as this corresponds to higher alkyl chain densities, increasing the steric penalty for headgroup insertion. This effect was indeed observed for DSPE. At 60 °C, the half-life for DSPE flip-flop varies from 35 min at 15 mN/m to 193 min at 30 mN/m (Table 1). The trend to slower rates at higher pressures is ubiquitous for all of the pure DSPE and DSPC bilayers studied here. The lipid packing also plays an important role in the flip-flop of DSPE + DSPC mixtures.

Flip-Flop Kinetics in DSPE+DSPC Bilayers. The kinetic results for mixed DSPE+DSPC bilayers produced several interesting findings. For those mixed bilayers where both the DSPE and DSPC components were characterized (x_{DSPE} = 0.25, 0.50, and 0.75), the kinetics of flip-flop for the two species were found to be indistinguishable, as determined from the fits to their Arrhenius plots. The correspondence of the kinetics for each species in the mixture is somewhat surprising, as it is commonly thought that each phospholipid in such a mixture will transfer with its own distinct rate (*9*, *33*). Another interesting observation can be made in regard to the variation in flip-flop rates as a function of membrane composition. The kinetics for flip-flop in bilayers at x_{DSPE} = 0.10 are markedly faster than for pure DSPC. This result is somewhat surprising, as it would be reasonable to assume the kinetic rates of flip-flop for the mixtures would fall somewhere between the pure components. As the mole fraction of DSPE is increased beyond 10%, the flip-flop kinetics for both DSPC and DSPC became slower as expected.

As noted in the Results section, the mean molecular area for these mixtures followed the same general trend. It has also been noted that the kinetics of flip-flop in the case of pure DSPE and DSPC bilayers is strongly dependent on the packing in the membrane, as evidenced by their pressure dependence. This evidence would suggest that the kinetics of flip-flop in these mixtures are primarily dependent on the packing in the membrane. However, there are a number of other factors which must be characterized as well if one is to determine the extent to which packing is responsible for the observed kinetics. These include the potential role of hydrogen bonding, headgroup polarity, and headgroup−solvent interaction on the flip-flop of DSPE relative to DSPC. The effect of each of these types of interactions, as well as the role of lipid packing, may be assessed using transition state theory. We first examine the thermodynamics which govern flip-flop of the pure DSPE and DSPC systems and subsequently apply these findings to the mixed systems.

Activation Thermodynamics of DSPE Flip-Flop. Comparison of the activation thermodynamics of flip-flop for DSPE and DSPC provides a direct measure of the influence of headgroup chemistry on the thermodynamic barrier to flipping. The data presented in Table 1 may be used to calculate the activation thermodynamics for pure DSPE, as has previously been done for DSPC (*45*). Using eq 7, we calculate the net free energy barrier for DSPE flip-flop at 30 mN/m to range from $\Delta G^{\ddagger}$ = 110.5 ± 0.4 kJ/mol at 60 °C to 107.0 ± 0.2 kJ/mol at 70.0 °C. Here, and in

Table 3: Activation Thermodynamics for Flip-Flop of 30 mN/m DSPE Bilayers at Several Temperatures[a]

temp (°C)	E_a (kJ/mol)	$\Delta a^{\ddagger}$ (Å^2/molecule)	$\Pi\Delta a^{\ddagger}$ (kJ/mol)	$\Delta H^{\ddagger}$ (kJ/mol)	$\Delta S^{\ddagger}$ (J/(mol K))	$T\Delta S^{\ddagger}$ (kJ/mol)	$\Delta G^{\ddagger}$ (kJ/mol)
DSPE							
50	231 ± 9	54 ± 5	9.7 ± 0.9	238 ± 9	328 ± 27	123 ± 9	114.0 ± 0.4
60	231 ± 9	52 ± 3	9.4 ± 0.5	238 ± 9	381 ± 27	127 ± 9	110.5 ± 0.2
70	231 ± 9	48 ± 4	8.7 ± 0.8	237 ± 9	380 ± 27	130 ± 9	107.0 ± 0.2
DSPC							
50	228 ± 28	31 ± 14	5.6 ± 2.5	231 ± 28	400 ± 80	130 ± 28	102 ± 1

[a]The activation thermodynamics for flip-flop of DSPC at 30 mN/m is provided for comparison and is taken from previous studies (*40*, *45*).

the sections that follow, we wish to compare the thermodynamics for DSPE flip-flop to our previous results for DSPC in order to examine the underlying physical and chemical factors possibly contributing to the differences in the flip-flop behavior of these two lipid species. To facilitate that comparison, we have examined the kinetics and thermodynamics of DPSC and DSPE flip-flop at a common temperature, 50.0 °C, at which both lipid species are in the gel state. This choice of temperature requires the extrapolation of the data for DSPE, as flip-flop of DSPE at 50.0 °C is too slow for practical direct measurement ($t_{1/2}$(calc) ~1.6 days). When calculated at the lower temperature of 50.0 °C, the net free energy barrier for DSPE flip-flop is $\Delta G^{\ddagger} = 114.0 \pm 0.4$ kJ/mol, while for DSPC the barrier is $\Delta G^{\ddagger} = 102 \pm 1$ kJ/mol, a difference of 12 kJ/mol. Taken alone, the total free energy barrier for DSPE flip-flop does not provide many clues about the differences in the nature of the transition state for DSPC and DSPE.

The presence (DSPC) or absence (DSPE) of methyl groups on the headgroup amine leads to differences in the size, hydrogen-bonding capacity, and hydrophobicity, and each of those factors is expected to alter the transition state thermodynamics in a different manner. For instance, hydrogen-bonding interactions between lipid groups might stabilize the ground state and increase the enthalpic barrier to flip-flop, while changes in hydrophobicity or solvent interaction may instead appear as an altered entropic barrier to lipid exhange (*58*). Examination of the energetic contributions to the net free energy barrier from entropy, enthalpy, and pressure work provides essential clues about the nature of the transition state and its dependence upon the chemical and physical properties of the membrane.

Activation Area and Pressure Work for DSPE Flip-Flop. The activation area provides a measure of the geometric constraints acting on a lipid molecule during flip-flop and is used to determine the pressure work which must be exerted on the surrounding system to accommodate the change in lipid geometry as it proceeds to the transition state. The activation area is determined by the dependence of the flip-flop rate on lateral pressure *at a fixed temperature*. However, the experimental method places practical limits on the range over which kinetic data which can be measured, as noted above. Therefore, it was not practical to measure the rate of flip-flop over the same range of temperatures for each pressure examined. Instead, the Arrhenius rate data (see Figure 4) are used to calculate the rates for each pressure at a common temperature. Using the calculated rates, the pressure-dependent thermodynamics may be determined at any temperature, within reason.

The activation area for DSPE is calculated from the data in Figure 4 by fitting to eq 10, where the fit was weighted for the error in each data set. The activation area for DSPE varies from 54 ± 5 Å^2/molecule at 50 °C to 48 ± 4 Å^2/molecule at 70 °C; the temperature dependence of $\Delta a^{\ddagger}$ for DSPE is listed in Table 3. The area per DSPE molecule undergoing flip-flop at 50 °C increases an average of 54 Å^2/molecule from the area occupied in the ground state (38.4 ± 0.6 Å^2/molecule), reaching an average total area of 93 ± 5 Å^2/molecule in the transition state geometry. A DSPE molecule undergoing flip-flop occupies more than double the area in the transition state than it had occupied in the ground state. This is consistent with, although not indicative of, a unimolecular mechanism for flip-flop wherein the lipid molecule is bent back along itself during the transition. Under the same conditions DSPC has a ground state area of 45.9 ± 1.4 Å^2/molecule, an activation area of 31 ± 14 Å^2/molecule, and a total transition state area of 77 ± 14 Å^2/molecule (*45*). The transition state areas differ slightly (at an 89% confidence interval), indicating that DSPE occupies slightly more space in the membrane during flip-flop than DSPC, in spite of a higher packing density in the ground state. Thus the larger activation area for DSPE most likely arises from both a decrease in the ground state area per molecule and an increase in the area occupied at the transition state.

The larger activation area also indicates that more work must be done on the surrounding lipids in order to achieve this configuration. For DSPE at 30 mN/m and 50 °C, the reversible pressure work required to reach the transition state, given as $\Pi\Delta a^{\ddagger}$, is 9.7 ± 1 kJ/mol. The work required for DSPC under these conditions is slightly smaller, at 5.6 ± 2.5 kJ/mol. This indicates that more energy is required to create the necessary space for a lipid to assume the transition state geometry in the tightly packed DSPE membrane than in a DSPC membrane. It should be noted that while the difference in the work term for these two species is 4.1 kJ/mol, less than half of this additional energy (1.0−1.7 kJ/mol) can be directly attributed to the change in ground state packing alone. The amount of work attributed to ground state packing differences was calculated using $\Pi\Delta a_{0_{DSPC-DSPE}}$, where $\Delta a_{0_{DSPC-DSPE}}$ is the difference in ground state areas for the two lipid species. For the lipids considered here, this turns out to be 1.0−1.7 kJ/mol. The remaining difference in the work term for DSPC and DSPE can be attributed to differences in the transition state geometry rather than the ground state geometry, suggesting that DSPE adopts a larger molar transition state area than DSPC (using the $\Pi-a$ isotherm data as an estimate of ground state packing).

Activation Enthalpy for DSPE Flip-Flop. Differences in the enthalpic barrier to DSPE and DSPC flip-flop may also provide unique information about the different mechanisms for flip-flop of these two lipid species. The sources of enthalpy in the

system arise from hydrogen bonding, electrostatic interactions, and van der Waals interactions. The enthalpic barrier to flip-flop arises from the loss of these favorable interactions between lipid molecules or between lipid and solvent as flip-flop occurs. It is generally assumed that the identity of the headgroup will significantly affect the enthalpy barrier by altering these stabilizing interactions, while other properties such as alkyl chain length, structure, and order are more closely related to the entropic portion of the energy barrier (*9*, *45*). The work term, in conjunction with the Arrhenius activation energy E_a, may be used to determine the total activation enthalpy barrier for DSPE flip-flop as

$$\Delta H^{\ddagger} = E_a - RT + \Pi \Delta a^{\ddagger} \quad (14)$$

From the Arrhenius plot shown in Figure 4, E_a for DSPE at 30 mN/m was calculated to be 231 ± 9 kJ/mol. The Arrhenius activation energy is within error of that previously determined for DSPC (228 ± 28 kJ/mol) and its shorter chain analogues (*40*). Using E_a along with the work term, $\Delta H^{\ddagger}$ for DSPE was calculated to be 238 ± 9 kJ/mol at 50.0 °C. For DSPC under the same conditions, $\Delta H^{\ddagger}$ is calculated to be 231 ± 28 kJ/mol. The net enthalpy barrier for DSPE flip-flop is indistinguishable from that for DSPC, given the errors in the measurement.

Based on these data it appears that the chemical differences in DSPE and DSPC, namely, the ability of DSPE to act as a hydrogen bond donor, do not significantly alter the enthalpic penalty for reaching the transition state. This result is somewhat surprising, as interlipid hydrogen bonding between DSPE molecules should stabilize the lipids in the ground state and increase the enthalpy required for adopting a transition state geometry. This effect is observed in the case of desorption of a lipid from vesicles in solution (*59*). The energy barrier for desorption of a short-chained fluorescent lipid probe bearing a phosphoethanolamine headgroup (C_6-NBD-PE) from a POPC matrix was found to be approximately 2.8 kJ/mol higher than that for a related phosphocholine analogue (C_6-NBD-PC) (*59*). In pure DSPE bilayers this effect might be up to twice as large, due to the capacity for the matrix molecules to act as both hydrogen bond acceptors and hydrogen bond donors. This process is mechanistically different from flip-flop but provides some measure of the relative differences in intermolecular bonding for phosphoethanolamines and phosphocholines. However, small energetic differences such as these (2−4 kJ/mol) are insignificant in relation to the exceedingly large net activation enthalpy (231 ± 9 kJ/mol) and the error in their determination. It should be noted that the measurement errors in $\Delta H^{\ddagger}$ for flip-flop are a direct consequence of the limited temperature range over which these bilayer systems can be studied.

Activation Entropy for DSPE Flip-Flop. From the kinetic data presented above, it is also possible to examine the role of entropy in determining the net free energy barrier to flip-flop. The activation entropy represents the difference in entropy between a DSPE lipid in the transition state geometry and the same lipid in the ground state geometry. Using eq 11, the activation entropy for DSPE at 50 °C and 30 mN/m was calculated to be 380 ± 27 J/(mol K). These data, along with the calculated activation entropy for DSPE flip-flop at 60.0 and 70.0 °C, are presented in Table 3. A positive $\Delta S^{\ddagger}$ indicates that the entropy of the system increases during the flipping event. This result is fairly intuitive as the ground state for a gel phase lipid is very well ordered with few gauche defects in the alkyl chain and little penetration of polar solvent into the hydrophobic core. The change in geometry required for flip-flop to occur involves the rearrangement of the surrounding lipid molecules in order to accommodate the larger area of the transition state lipid as the polar headgroup is inserted into the lipid bilayer, all of which are correlated with positive changes in entropy. Changes in the hydration of the headgroup during flip-flop or ordering of the solvent due to exposure of the alkyl chains will also have a significant effect on the entropy of the system. The activation entropies for DSPE and DSPC were compared in order to better understand the structural factors underlying the observed thermodynamic behavior.

At 50.0 °C, the activation entropy for DSPC is 400 ± 80 J/mol, higher than that for DSPE. For DSPE, the entropic portion of the free energy barrier is $T\Delta S^{\ddagger}$ = 123 ± 9 kJ/mol. For comparison, $T\Delta S^{\ddagger}$ for DSPC is calculated to be 130 ± 28 kJ/mol under the same conditions. The entropy and enthalpy terms contribute to the free energy barrier with opposite sign, meaning that the entropic contribution is favorable and partially compensates for the large enthalpic barrier to flip-flop. In terms of its effect on the free energy barrier, the favorable entropic contribution to the barrier is reduced for DSPE relative to DSPC. The reduced activation entropy for DSPE may be due to either an increase in the ground state entropy or a decrease in the transition state entropy relative to DSPC. The pressure−area isotherms presented above indicate that DSPE is more tightly packed in the ground state than DSPC. Based on these geometric considerations, the ground state entropy for DSPE bilayers is expected to be significantly lower than for DSPC if only the contribution from the lipid molecules is considered and the effect of solvent molecules is neglected. The larger activation area for DSPE also indicates that greater rearrangement of the lipid molecules is required to reach the transition state, which suggests greater disparity between the order of the lipid alkyl chains in the ground and transition states for DSPE relative to DSPC. This greater disparity in order should translate to a higher activation entropy for DSPE, contrary to our observation. Thus the lipid packing and lipid chain order alone cannot explain the decrease in activation entropy associated with the change in headgroup chemistry. This would suggest that the decreased activation entropy for DSPE may instead reflect the behavior of the water associated with the lipids at the interface. This effect can be better understood by considering the structure of the water molecules which surround the ethanolamine and choline headgroups, respectively. For simplicity, only the solvent interactions with the terminal region of the headgroup are considered, as the remaining portions of the molecules are essentially identical. For the choline headgroup, the water molecules arrange in a clathrate-like structure in order to minimize their contact with the hydrophobic methyl groups bound to the nitrogen moiety (*60*). The ethanolamine headgroup lacks these methyl groups and is capable of hydrogen bonding with the solvent and, thus, does not induce the same degree of solvent rearrangement. One manifestation of this effect is the difference in the number of water molecules directly involved in the hydration of the two headgroups (including phosphate and carbonyl groups etc.) which ranges from 7−8 molecules to 12−30 molecules for PE and PC, respectively (*61*−*63*). This effect is most readily understood as a consequence of the relative hydrophobicity of these two headgroups. Because a greater number of water molecules are induced to reorder around the more hydrophobic choline headgroup, this headgroup will have a greater effect on the solvent entropy than the smaller and more hydrophilic ethanolamine moiety. The

impact of headgroup hydrophobicity on the activation thermodynamics for lipid flip-flop is examined in greater detail below.

Influence of Headgroup Hydrophobicity on the Thermodynamics of Flip-Flop. It is possible to estimate how the hydrophobicity of a lipid headgroup will influence the thermodynamic barrier to flip-flop using available data in the literature. We can relate the movement of a lipid headgroup from the polar membrane exterior into the hydrophobic membrane interior to the partitioning of a polar solute between an aqueous and hydrocarbon phase. In extensive studies on the thermodynamics for transfer of various long-chain amphiphiles between water and various hydrocarbon phases, Tanford observed a dependence of ~3.4 kJ/mol per CH_2 unit transferred (*58*). By placing three methyl units on the amine of the ethanolamine headgroup, the additional thermodynamic driving force (preference of the headgroup for the hydrocarbon phase) would be approximately 10.3 kJ/mol, accounting for the additional methyl groups as methylene units. A refinement of this approach involves calculation of the magnitude of the hydrophobic interaction per surface area of the methyl groups, which is found to be approximately 88 J/(mol Å^2) (*64*). For a choline headgroup with a surface area of 118 Å^2 (*65*) the hydrophobic interaction would be approximately 10.4 kJ/mol, in good agreement with the estimate using the transfer energies of a single methylene unit.

It is worth restating that the hydrophobic effect involves the disruption of strong intermolecular interactions between water molecules due to the introduction of a solute, as well as the resulting reorganization of the water molecules to minimize this perturbation (*58*). If the solute is nonpolar, the water molecules will reorder in such a way as to minimize their interaction with the solute and maximize their interaction with other water molecules. This leads to ordering of the water molecules around the solute, producing a significant loss of solvent entropy. This is consistent with the increased activation entropy measured for DSPC relative to DSPE. The more hydrophobic choline headgroup induces ordering of the surrounding solvent, as evidenced by the clathrate-like arrangement of water molecules near the methyl groups (*60*). DSPE is able to better satisfy the hydrogen-bonding requirements of the solvent and does not induce the same degree of order (*60*). The importance of solvent entropy is also observed in other systems involving the hydrophobic effect, such as the folding of a protein in an aqueous environment (*66*). Because the number of solvent molecules involved is so great, minor changes in solvent entropy can have significant net contributions to the entropy of the system. This is due to the fact that the total entropy of the system scales with the number of atoms present (*67*).

Summary of DSPE Activation Thermodynamics. The various activation thermodynamic parameters determined here for DSPE flip-flop are summarized in Table 3. In spite of the alteration of the lipid headgroup chemistry, the activation enthalpies for DSPE and DSPC are nearly identical. However, the contributions to $\Delta H^{\ddagger}$ from the activation area and work terms are larger for DSPE, reflecting the smaller ground state area occupied by this lipid as a consequence of its smaller headgroup. The alteration of the headgroup chemistry is also apparent in the activation entropy for DSPE flip-flop, which is smaller than the activation entropy for DSPC flip-flop in spite of the larger geometric rearrangement required for DSPE. The total difference in the free energy barrier for DSPE and DSPC flip-flop is 12 kJ/mol. This difference in free energy can be attributed primarily to differences in the entropy of activation and pressure work required for flip-flop of DSPE or DSPC, while the difference in activation enthalpy was insignificant. Physically, these thermodynamic differences can be explained in terms of the decreased hydrophobicity and size of the ethanolamine headgroup, relative to DSPC, which lead to significantly different membrane packing and interfacial solvent structure for bilayers of these two lipids. On the basis of the differences in hydrophobicity of DSPE and DSPC alone, one would estimate a $\Delta\Delta G^{\ddagger}$ for flip-flop of 10.4 kJ/mol, in reasonable agreement with the observed difference of 12 kJ/mol. Moreover, the predicted differences in activation free energy due to the reduced hydrophobicity of DSPE would be primarily entropic in nature, consistent with our findings.

Table 4: Gibbs Free Energy of Activation for Mixed DSPE−DSPC Bilayers at Various DSPE Concentrations[a]

bilayer composition (LB layer)	$\Delta G^{\ddagger}$ (kJ/mol)
$\chi_{DSPC} = 0.90 - \chi_{DSPE\text{-}d_{70}} = 0.10$	97.4 ± 0.4
$\chi_{DSPC} = 0.75 - \chi_{DSPE\text{-}d_{70}} = 0.25$	103.5 ± 0.2
$\chi_{DSPE} = 0.25 - \chi_{DSPC\text{-}d_{70}} = 0.75$	102.5 ± 0.2
$\chi_{DSPC} = 0.50 - \chi_{DSPE\text{-}d_{70}} = 0.50$	105.9 ± 0.2
$\chi_{DSPE} = 0.50 - \chi_{DSPC\text{-}d_{70}} = 0.50$	105.7 ± 0.2
$\chi_{DSPC} = 0.25 - \chi_{DSPE\text{-}d_{70}} = 0.75$	109.3 ± 0.8
$\chi_{DSPE} = 0.75 - \chi_{DSPC\text{-}d_{70}} = 0.25$	108.3 ± 1.1
$\chi_{DSPE} = 1.00$	114.0 ± 0.4

[a]All values were calculated at 30 mN/m and 50 °C using the kinetic data presented in Table 2.

Activation Thermodynamics of Flip-Flop for Mixed DSPE + DSPC Bilayers. The activation thermodynamic analysis of DSPE and DSPC in single component membranes provides significant insight into the factors which govern their flip-flop in a homogeneous bilayer. We can also characterize the free energy barrier to flip-flop in binary mixtures of these lipids in order to understand the complex dependence of flip-flop kinetics on composition and packing. The free energy of activation for each mixture was calculated according to eq 7, where the kinetic data for each mixture were extrapolated to a common temperature assuming Arrhenius behavior. The calculation of the free energy barrier at a common temperature is essential for comparison of the data, as $\Delta G^{\ddagger}$ is highly dependent on temperature and lipid phase. The choice of temperature in this case was 50 °C, as this temperature requires a minimal degree of extrapolation for the kinetic data collected and facilitates comparison with the pure bilayer systems discussed above. The free energies of activation calculated at 50 °C for DSPE + DSPC mixed bilayers are summarized in Table 4.

The Gibbs free energy barrier, $\Delta G^{\ddagger}$, for each component of the mixed bilayers will be considered in turn, beginning with DSPC. At $x_{DSPE} = 0.10$, the free energy barrier for DSPC flip-flop is only 97.4 ± 0.4 kJ/mol, which is considerably lower than the barrier to flip-flop in pure DSPC bilayers (102 ± 1 kJ/mol) at the same temperature. As previously mentioned, the flip-flop of DSPE in these mixtures could not be determined due to the low SFVS signal at low lipid densities. As x_{DSPE} increased, the activation free energy barrier increased with values of 103.5 ± 0.2, 106.0 ± 0.2l, and 109.3 ± 0.8 kJ/mol calculated for DSPC flip-flop in bilayers containing $x_{DSPE} = 0.25$, 0.50, and 0.75, respectively. These data highlight the odd behavior of bilayers with $x_{DSPE} = 0.10$. The barrier to DSPC flip-flop decreases ~4.6 kJ/mol when DSPE is initially introduced into the bilayer, in spite of the fact that pure DSPE flip-flop has a free energy barrier that is 12 kJ/mol greater than DSPC. Similar results are observed for the DSPE component of the mixed bilayers at 50.0 °C.

$\Delta G^{\ddagger}$ values of 102.5 ± 0.3, 105.7 ± 0.2, and 108.3 ± 1.1 kJ/mol were calculated for DSPE flip-flop in bilayers containing DSPE mole fractions of 0.25, 0.50, and 0.75, respectively. For comparison, the free energy of activation for DSPC and DSPE flip-flop in the mixed bilayers is summarized in Table 4.

At those mole fractions where both the DSPE and DSPC components were characterized, the free energy barrier to DSPE flip-flop was essentially indistinguishable from that for DSPC, consistent with the kinetic results presented earlier. (Note: The difference appears statistically significant at $x_{DSPE} = 0.25$ DSPE, but the sample size is small.) This is illustrated in Figure 8, where the free energy barriers to DSPE and DSPC flip-flop in mixed DSPE + DSPC bilayers are shown as a function of membrane composition. The similarity in the free energy barrier for each component in a given mixture might then suggest that both lipids have similar $\Delta H^{\ddagger}$, $\Delta S^{\ddagger}$, and $\Pi \Delta a^{\ddagger}$ terms. For the work term, this is an intuitive result, as mixtures of these lipids are completely miscible (*43*), leading to identical local environments for each lipid molecule. Thus the ground state packing and the work required to displace neighboring lipids molecules should be nearly identical for each species. If the work terms are similar, then the differences in the enthalpic contributions to the energy barrier, which are already insignificant, would be further reduced. The similarity in local packing constraints would also somewhat minimize the differences in activation entropy between the two lipid species; however, it would be reasonable to expect that $\Delta S^{\ddagger}$ for DSPE and DSPC should still differ slightly due to their differing hydrophobicities and headgroup solvation. It is also possible that the enthalpic barrier to DSPE is reduced in the presence of DSPC due to the loss of DSPE−DSPE hydrogen bonding. This effect may compensate for any differences in the activation entropy barrier for flip-flop of these two lipid species. However, changes in $\Delta H^{\ddagger}$ due to hydrogen bonding would be concentration dependent and are not consistent with our observation that both DSPE and DSPC show similar energetic barriers to one another in their mixtures over a large range of compositions (see Figure 8).

Based on the miscibility of DSPE + DSPC mixtures and the strong influence of molecular packing on the similar transition state thermodynamics of the pure lipid components, similar, if not identical, free energy barriers can be rationalized for DSPE and DSPC in the binary mixture. The better than expected agreement in $\Delta G^{\ddagger}$ for these species may be due to a serendipitous balance of the enthalpy and entropy terms as hydration and hydrogen bonding change with composition or may reflect changes in solvent ordering within the mixtures that have yet to be described in the literature.

At first glance, it would appear that the hydrophobicity of the lipid headgroup is not as good an indicator of the activation thermodynamics and flip-flop rates in mixed bilayers as we found for the pure bilayers. However, it is important to note that the hydrophobicity of the molecule determines the orientation and solvent structure of the headgroup and therefore strongly influences the molecular packing of the lipids in the bilayer (*65*), a physical property which is more clearly correlated to the thermodynamic behavior of the mixtures.

The role of lipid packing as a primary determinant of the thermodynamic behavior for these mixtures can be readily established based on the seemingly identical trends observed for the free energy barrier and molecular packing densities of the mixed bilayers as a function of composition. By graphing the free energy barrier for flip-flop at 30 mN/m and 50.0 °C in

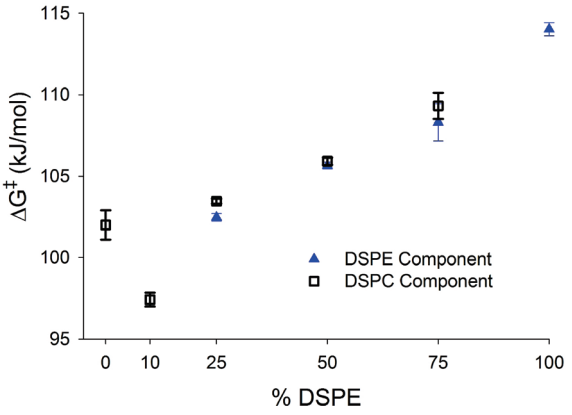

FIGURE 8: Free energy of activation for mixed DSPE−DSPC bilayers as a function of DSPE concentration. Open squares refer to the DSPC component of the mixed bilayers while closed triangles refer to the DSPE component.

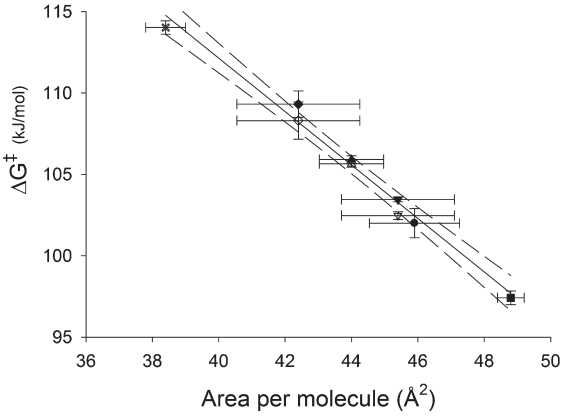

FIGURE 9: Activation free energy for mixed DSPE−DSPC bilayers as a function of mean molecular area, as determined from the data presented in Figures 7 and 8. Solid symbols refer to the DSPC component of mixed bilayers while open symbols refer to the DSPE component. The concentrations shown are 100% DSPC (0% DSPE) (circle), 10% DSPE (square), 25% DSPE (triangles down), 50% DSPE (triangles up), 75% DSPE (diamonds), and 100% DSPE (×).

DSPE + DSPC mixtures as a function of the area per molecule in those bilayers, the dependence of the free energy barrier on the membrane packing can be clearly seen (Figure 9). Figure 9 also illustrates the fact that complex compositional dependence of the free energy barrier to lipid flip-flop in DSPE + DSPC bilayers may be fully described in terms of the molecular packing alone. While it appears that the packing of the lipids in the membrane is a primary determinant of the energetic barrier to flip-flop for DSPE + DSPC mixtures, the dependence of the area per lipid molecule on DSPE concentration is not a simple one. However, the seemingly anomalous increase in mean molecular area at 10% DSPE in DSPC has been previously observed for mixed DSPE + DSPC monolayers at elevated temperatures (35−40 °C), although this trend was reversed at lower temperatures (25 °C) (*43*). As was observed in our present work, those authors noted an initial expansion of the film near $x_{DSPE} = 0.10$ and a subsequent decrease in mean molecular area at higher mole fractions of DSPE (*43*). The deviations from ideal packing behavior were greatest for $x_{DSPE} = 0.10$ and $x_{DSPE} = 0.90$ (or $x_{DSPC} = 0.10$, equivalently), where the attractive and repulsive forces are most imbalanced (*43*). The authors suggested that the interplay between hydration forces and dispersion forces was

primarily responsible for the observed dependence on concentration and temperature (*43*). When DSPE is introduced into DSPC at low concentrations (10%), the electrostatic repulsion may dominate the interaction between neighboring lipids while the dispersion interactions (between the acyl chains) resemble that of pure DSPC films (weaker dispersion forces than DSPE due to increased separation). This would lead to a net increase in the area per molecule at low DSPE concentrations that is recovered as the DSPE concentration increases. It is possible that such a scenario describes the packing trends observed in the mixed monolayers considered here or that the effect is more directly related to the availability of hydrogen bond donors in bilayers with low DSPE concentration. It should be emphasized that the variation in molecular area for DSPE + DSPC bilayers of differing concentrations is not fully understood at this time. Nonetheless, it is clear from the data shown in Figure 9 that the free energy barrier to flip-flop is strongly dependent on the resultant area per molecule.

Review of Factors Governing Flip-Flop in Mixed DSPE + DSPC Bilayers. It has long been thought that the chemistry of the headgroup would determine, in large part, the nature of the thermodynamic barrier for flip-flop (*9*, *33*). Our findings have shown that each component of the DSPE−DSPC bilayer undergoes flipping with a common rate and energetic barrier that is characteristic of the gross structural properties of the membrane rather than the identity of the lipid molecule. Specifically, the data presented in Figure 9 suggest that the thermodynamics of DSPE + DSPC mixtures are well described by their packing characteristics alone. This result reflects the miscibility of the lipid species, as the local environments for each species are identical. The components in mixed bilayers which are not fully miscible would be expected to deviate from the behavior observed here for DSPE + DSPC, likely exhibiting disparate rates and thermodynamics of flip-flop. Phase-segregated lipid molecules would experience significantly different local environments, and their flip-flop activation thermodynamics may reflect that disparity.

Kol et al. studied the dependence of lipid flip-flop rate of a fluorescently labeled lipid probe on the composition of vesicles containing small transmembrane peptides, which are known to facilitate spontaneous flip-flop. The facilitated flip-flop of the lipid probe was strongly inhibited by the incorporation of cholesterol into the membrane. The authors attributed this effect to the ordering effect of cholesterol in liquid phase vesicles and the increase in local chain packing (*68*). This is consistent with our findings that the local packing arrangement of the lipid molecules in the bilayer will strongly affect the net free energy barrier to flip-flop.

It should also be noted that it is not yet clear whether a simple area dependence for the thermodynamics of flip-flop should be expected for lipid mixtures where greater disparity in headgroup chemistry is present. For instance, lipids with a serine-derived headgroup, bearing a net negative charge at neutral pH, may exhibit entirely different flip-flop behavior from their neutral counterparts, particularly with respect to the enthalpic barrier to flip-flop. NMR studies on the interaction of different headgroups in mixed bilayers have indicated that charged headgroups interact more strongly with zwitterionic lipids (PE or PC) than is found in the simple PE−PC mixtures (*69*). Further study of additional lipid mixtures will be required to characterize the flip-flop behavior of such species, and preliminary work is underway in our laboratory to address this possibility.

CONCLUSIONS

Our findings suggest that the local packing of the lipid molecules within a bilayer is an important determinant of the kinetics and thermodynamics of flip-flop. The chemical identity of the lipid headgroup, either phosphocholine or phosphoethanolamine, is found to profoundly influence the kinetics and thermodynamics of flip-flop in pure lipid bilayers, primarily by altering the lipid packing and lipid−solvent interactions within the bilayer. Specifically, the relative size and hydrophobicity of the headgroups largely explain the differences in activation thermodynamics for the two lipids. In mixtures of DSPE and DSPC, both species undergo exchange at similar rates and experience similar activation thermodynamic barriers. The thermodynamic barrier to flip-flop for these lipids did not, however, vary smoothly with membrane composition. Instead, the energetic barrier to flip-flop was strongly correlated to the area per molecule for the mixed bilayers.

We have also shown that SFVS is uniquely capable of independently describing each component of a complex mixture by careful selection of the appropriate deuterated or protiated lipid species. To our knowledge, this study represents the first such independent determination of the kinetics of different native lipid species within binary mixtures without the use of chemically modified probes.

Additional study of the dynamics of lipid mixtures by this method will provide a unique opportunity to further characterize the mechanisms for spontaneous lipid flip-flop in PSLBs. It is of particularly great interest to determine whether the common behavior of all lipid components within the mixture is a ubiquitous property of bilayers consisting of miscible species or if this is a unique aspect of the DSPE + DSPC system. Such information will provide an important window onto the possible mechanisms involved in the spontaneous flip-flop of lipid molecules within the bilayer.

REFERENCES

1. Devlin, T. M. (1997) Textbook of Biochemistry with Clinical Correlations , 4th ed., Wiley, New York.
2. Meer, G. v., Voelker, D. R., and Feigenson, G. W. (2008) Membrane lipids: where they are and how they behave. *Nature Rev. Mol. Cell Biol. 9*, 112–124.
3. Devaux, P. F. (1993) Lipid transmembrane asymmetry and flip-flop in biological membranes and in lipid bilayers. *Curr. Opin. Struct. Biol. 3*, 489–494.
4. Bretscher, M. S. (1973) Membrane structure: some general principles. *Science 181*, 622–629.
5. Marsh, D. (1990) CRC Handbook of Lipid Bilayers , CRC Press, Boca Raton, FL.
6. Seu, K. J., Cambrea, L. R., Everly, R. M., and Hovix, J. S. (2006) Influence of lipid chemistry on membrane fluidity: tail and headgroup interactions. *Biophys. J. 91*, 3727–3735.
7. Mathai, J. C., Tristam-Nagle, S., Nagle, J. F., and Zeidel, M. L. (2008) Structural determinants of water permeability through the lipid membrane. *J. Gen. Physiol. 131*, 69–76.
8. Nagle, J. F., Mathai, J. C., Zeidel, M. L., and Tristam-Nagle, S. (2008) Theory of passive permeability through lipid bilayers. *J. Gen. Physiol. 131*, 77–85.
9. Homan, R., and Pownall, H. J. (1988) Transbilayer diffusion of phospholipids: dependence on headgroup structure and acyl chain length. *Biochim. Biophys. Acta 938*, 155–166.
10. Kol, M. A., de Kroon, A. I. P. M., Killian, J. A., and de Kruijff, B. (2004) Transbilayer movement of phospholipids in biogenic membranes. *Biochemistry 43*, 2673–2681.
11. Kol, M. A., de Kruijff, B., and de Kroon, A. I. P. M. (2002) Phospholipid flip-flop in biogenic membranes: what is needed to connect opposite sides. *Semin. Cell Dev. Biol. 13*, 163–170.
12. Balasubramanian, K., and Schroit, A. J. (2002) Aminophospholipid asymmetry: a matter of life and death. *Annu. Rev. Physiol. 65*, 701–734.

13. Bretscher, M. S. (1972) Asymmetrical lipid bilayer structure for biological membranes. *Nat. New Biol. 236*, 11–12.
14. Devaux, P. F., and Zachowski, A. (1994) Maintenance and consequences of membrane phospholipid asymmetry. *Chem. Phys. Lipids 73*, 107–120.
15. Kornberg, R. D., and McConnell, H. M. (1971) Lateral diffusion of phospholipids in a vesicle membrane. *Proc. Natl. Acad. Sci. U.S.A. 68*, 2564–2568.
16. Zwaal, R. F. A., and Schroit, A. J. (1997) Pathophysiological implications of membrane phospholipid asymmetry in blood cells. *J. Am. Soc. Hematol. 89*, 1121–1132.
17. Bevers, E. M., Comfurius, P., Dekkers, D. W. C., and Zwaal, R. F. A. (1999) Lipid translocation across the plasma membrane of mammalian cells. *Biochim. Biophys. Acta 1439*, 317–330.
18. Pomorski, T., and Menon, A. K. (2006) Lipid flippases and their biological functions. *Cell. Mol. Life Sci. 63*, 2908–2921.
19. Daleke, D. L., and Lyles, J. V. (2000) Identification and purification of aminophospholipid flippases. *Biochim. Biophys. Acta 1486*, 108–127.
20. Herrmann, A., Zachowski, A., and Devaux, P. F. (1990) Protein-mediated phospholipid translocation in the endoplasmic reticulum with a low lipid specificity. *Biochemistry 29*, 2023–2027.
21. Vondenhof, A., Oslender, A., Deuticke, B., and Haest, C. W. M. (1994) Band 3, an accidental flippase for anionic phospholipids? *Biochemistry 33*, 4517–4520.
22. Huijbregts, R. P., de Kroon, A. I., and de Kruijff, B. (1998) Rapid transmembrane movement of newly synthesized phosphatidylethanolamine across the inner membrane of *Escherichia coli*. *J. Biol. Chem. 273*, 18936–18942.
23. Kornberg, R. D., and McConnell, H. M. (1971) Inside-outside transitions of phospholipids in vesicle membranes. *Biochemistry 10*, 1111–1120.
24. McConnell, H. M., and Hubbell, W. L. (1971) Molecular motion in spin-labeled phospholipids and membranes. *J. Am. Chem. Soc. 93*, 314–326.
25. Gallet, P. F., Zachowski, A., Julien, R., Fellmann, P., Devaux, P. F., and Maftah, A. (1999) Transbilayer movement and distribution of spin-labelled phospholipids in the inner mitochondrial membrane. *Biochim. Biophys. Acta 1418*, 61–70.
26. Rousselet, A., Colbeau, A., Vignais, P. M., and D., P. F. (1976) Study of the transverse diffusion of spin-labeled phospholipids in biological membranes. II. Inner mitochondrial membrane of rat liver: use of phosphatidylcholine exchange protein. *Biochim. Biophys. Acta 426*, 372–384.
27. Cabral, D. J., Small, D. M., Lilly, H. S., and Hamilton, J. A. (1987) Transbilayer movement of bile acids in model membranes. *Biochemistry 26*, 1801–1804.
28. John, K., Schreiber, S., Kubelt, J., Herrmann, A., and Muller, P. (2002) Transbilayer movement of phospholipids at the main phase transition of lipid membranes: implications for rapid flip-flop in biological membranes. *Biophys. J. 83*, 3315–3323.
29. Colleau, M., Herve, P., Fellmann, P., and Devaux, P. F. (1991) Transmembrane diffusion of fluorescent phospholipids in human erythrocytes. *Chem. Phys. Lipids 57*, 29–37.
30. Dekkers, D. W. C., Comfurius, P., Schroit, A. J., Bevers, E. M., and Zwaal, R. F. A. (1998) Transbilayer movement of nbd-labeled phospholipids in red blood cell membranes: outward-directed transport by the multidrug resistance protein 1 (MRP1). *Biochemistry 37*, 14833–14837.
31. Hrafnsdottir, S., Nichols, J. W., and Menon, A. K. (1997) Transbilayer movement of fluorescent phospholipids in *Bacillus megaterium* membrane vesicles. *Biochemistry 36*, 4969–4978.
32. Wimley, W. C., and Thompson, T. E. (1990) Exchange and flip-flop of dimyristoylphosphatidylcholine in liquid-crystalline, gel, and two-component, two-phase large unilamellar vesicles. *Biochemistry 29*, 1296–1303.
33. Wimley, W. C., and Thompson, T. E. (1991) Transbilayer and interbilayer phospholipid exchange in dimyristoylphosphatidylcholine/dimyristoylphosphatidylethanolamine large unilamellar vesicles. *Biochemistry 30*, 1702–1709.
34. Papadopulos, A., Vehring, S., López-Montero, I., Kutschenko, L., Stöckl, M., Devaux, P. F., Kozlov, M., Pomorski, T., and Herrmann, A. (2007) Flippase activity detected with unlabeled lipids by shape changes of giant unilamellar vesicles. *J. Biol. Chem. 282*, 15559–15568.
35. Roseman, M., Litman, B. J., and Thompson, T. E. (1975) Transbilayer exchange of phosphatidylethanolamine for phosphatidylcholine and N-acetimidoylphosphatidylethanolamine in single-walled bilayer vesicles. *Biochemistry 14*, 4826–4830.
36. Nakano, M., Fukuda, M., Kudo, T., Endo, H., and Handa, T. (2007) Determination of interbilayer and transbilayer lipid transfers by time-resolved small-angle neutron scattering. *Phys. Rev. Lett. 98*, 238101–238104.
37. Anglin, T. C., and Conboy, J. C. (2008) Lateral pressure dependence of the phospholipid transmembrane diffusion rate in planar-supported lipid bilayers. *Biophys. J. 95*, 186–193.
38. Anglin, T. C., Liu, J., and Conboy, J. C. (2007) Facile lipid flip-flop in a phospholipid bilayer induced by gramicidin A measured by sum-frequency vibrational spectroscopy. *Biophys. J. 92*, L01–L03.
39. Liu, J., and Conboy, J. C. (2004) Direct measurement of the transbilayer movement of phospholipids by sum-frequency vibrational spectroscopy. *J. Am. Chem. Soc. 126*, 8376–8377.
40. Liu, J., and Conboy, J. C. (2005) 1,2-Diacyl-phosphatidylcholine flip-flop measured directly by sum-frequency vibrational spectroscopy. *Biophys. J. 89*, 2522–2532.
41. Tokutake, N., Jing, B., Cao, H., and Regen, S. L. (2003) Quantifying the effects of deuterium substitution on phospholipid mixing in bilayer membranes. A nearest-neighbor recognition investigation. *J. Am. Chem. Soc. 125*, 15764–15766.
42. Liu, J., and Conboy, J. C. (2007) Asymmetric distribution of lipids in a phase segregated phospholipid bilayer observed by sum-frequency vibrational spectroscopy. *J. Phys. Chem. C 111*, 8988–8999.
43. Sánchez-González, J., Cabrerizo-Vilchez, M. A., and Gálvez-Ruiz, M. J. (1998) Chain dependence in phospholipid interactions: a thermodynamic study of mixed monolayers. *Colloid Polym. Sci. 276*, 239–246.
44. Liu, J., and Conboy, J. C. (2005) Structure of a gel phase lipid bilayer prepared by the Langmuir-Blodgett/Langmuir-Schaefer method characterized by sum-frequency vibrational spectroscopy. *Langmuir 21*, 9091–9097.
45. Anglin, T. C., Cooper, M. P., Li, H., Chandler, K., and Conboy, J. C. (2008) Free energy and entropy of activation for phospholipid flip-flop in planar supported lipid bilayers (manuscript in preparation).
46. Eyring, H. (1935) The activated complex and the absolute rate of chemical reactions. *Chem. Rev. 17*, 65–77.
47. Wynne-Jones, W. F. K., and Eyring, H. (1935) The absolute rate of reactions in condensed phases. *J. Chem. Phys. 3*, 492–502.
48. Homan, R., and Pownall, H. J. (1987) Effect of pressure on phospholipid translocation in lipid bilayers. *J. Am. Chem. Soc. 109*, 4759–4760.
49. Langmuir, I. (1933) Oil lenses on water and the nature of monomolecular expanded films. *J. Chem. Phys. 1*, 756–776.
50. Langmuir, I. (1936) Two-dimensional gases, liquids and solids. *Science 84*, 379–383.
51. Marsh, D. (1996) Lateral pressure in membranes. *Biochim. Biophys. Acta 1286*, 183–223.
52. Langmuir, I. (1917) The constitution and fundamental properties of solids and liquids. II. Liquids. *J. Am. Chem. Soc. 39*, 1848–1906.
53. Messmer, M. C., Conboy, J. C., and Richmond, G. L. (1995) Observation of molecular ordering at the liquid-liquid interface by resonant sum frequency generation. *J. Am. Chem. Soc. 117*, 8039–8040.
54. Conboy, J. C., Daschbach, J. L., and Richmond, G. L. (1994) Total internal reflection second-harmonic generation: probing the alkane water interface. *Appl. Phys. A: Solids Surf. A59*, 623–629.
55. Conboy, J. C., Messmer, M. C., and Richmond, G. L. (1996) Investigation of surfactant conformation and order at the liquid-liquid interface by total internal reflection sum-frequency vibrational spectroscopy. *J. Phys. Chem. 100*, 7617–7622.
56. Hine, J., and Thomas, C. H. (1953) Rate of deuterium exchange of certain amines and alcohols. *J. Am. Chem. Soc. 76*, 612–612.
57. McMullen, T. P. W., and McElhany, R. N. (1997) Differential scanning calorimetric studies of the interaction of cholesterol with distearoyl and dielaidoyl molecular species of phosphatidylcholine, phosphatidylethanolamine and phosphatidylserine. *Biochemistry 36*, 4979–4986.
58. Tanford, C. (1973) The hydrophobic effect: formation of micelles and biological membranes , John Wiley and Sons, New York.
59. Slater, S. J., Ho, C., Taddeo, F. J., Kelly, M. B., and Stubbs, C. D. (1993) Contribution of hydrogen bonding to lipid-lipid interactions in membranes and the role of lipid order: effects of cholesterol, increased phospholipid unsaturation, and ethanol. *Biochemistry 32*, 3714–3721.
60. Murzyn, K., Zhao, W., Karttunen, M., Kurdziel, M., and Róg, T. (2006) Dynamics of water at membrane surfaces: effect of headgroup structure. *Biointerphases 1*, 98–105.
61. Sen, A., and Hui, S.-W. (1988) Direct measurement of headgroup hydration of polar lipids in inverted micelles. *Chem. Phys. Lipids 49*, 179–184.

62. Cevc, G., and Marsh, D. (1985) Hydration of noncharged lipid bilayer membranes. *Biophys. J. 47*, 21–31.
63. Seddon, J. M., Cevc, G., Kaye, R. D., and Marsh, D. (1984) X-ray diffraction study of the polymorphism of hydrated diacyl- and dialkylphosphaidylethanolamines. *Biochemistry 23*, 2634–2644.
64. Reynolds, J. A., Gilbert, D. B., and Tanford, C. (1974) Empirical correlation between hydrophobic free energy and aqueous cavity surface area. *Proc. Natl. Acad. Sci. U.S.A. 71*, 2925–2927.
65. Dyck, M., Krüger, P., and Lösche, M. (2005) Headgroup organization and hydration of methylated phosphatidlyethanolamines in Langmuir monolayers. *Phys. Chem. Chem. Phys. 7*, 150–156.
66. Fisicaro, E., Compari, C., and Braibanti, A. (2004) Entropy/enthalpy compensation: hydrophobic effect, micelles and protein complexes. *Phys. Chem. Chem. Phys. 6*, 4156–4166.
67. Hill, T. L. (1986) An Introduction to Statistical Thermodynamics, Dover Publications, New York.
68. Kol, M. A., van Laak, A. N. C., Rijkers, D. T. S., Killian, J. A., de Kroon, A. I. P. M., and de Kruijff, B. (2003) Phospholipid flop induced by transmembrane peptides in model membranes is modulated by lipid composition. *Biochemistry 42*, 231–237.
69. Sixl, F., and Watts, A. (1983) Headgroup interactions in mixed phospholipid bilayers. *Proc. Natl. Acad. Sci. U.S.A. 80*, 1613–1615.